Characterization of sensitivity to finite perturbations

Tobias Letz* and Holger Kantz
Max-Planck-Institut für Physik komplexer Systeme
Nöthnitzer Str. 38, D 01187 Dresden, Germany
letz@uni-oldenburg.de, kantz@mpipks-dresden.mpg.de

We introduce a scale dependent stability number which describes the response of a dynamical system to finite size perturbations. By construction, it converges to the maximal Lyapunov exponent in the limit of infinitesimal perturbations. We discuss different dynamical systems which are linearly stable but unstable in terms of the finite size analysis. In such a situation typical trajectories can show temporal disorder, which has its origin in a kind of mixing on the mesoscopic scales.

5.45

I. INTRODUCTION

Commonly, chaos is defined by sensitive dependence on initial conditions, which, when the solution lives on a compact support, is synonymous with the existence of at least one positive Lyapunov exponent and a positive KS-entropy. Although it is well known that higher order terms in the stability analysis in principle might be relevant, in particular for marginally stable motion, it is common experience that the results of the linear stability analysis are in agreement with observations. Thus, motion with a zero or even negative maximal Lyapunov exponent is considered to be robust against perturbations and perturbations are known to grow at most algebraically in the former case. On the other hand, systems with a positive Lyapunov exponent display visible temporal disorder.

In time series analysis [1], where one tries to obtain the invariant quantities like Lyapunov exponents, entropies and dimensions from observed data rather than from numerical solutions of model equations, it is observed that the stability of motion on the infinitesimal scales generally can be well obtained from stability on finite length scales, as long as these scales are sufficiently smaller than the overall extension of the attractor. In particular, a positive maximal Lyapunov exponent is reflected by an exponential growth of distances between nearby trajectories with the correct exponent [2–4] up to scales delimited by the size of the attractor, where naturally saturation has to set in.

We will discuss several systems where the situation is dramatically different. Although the divergence of infinitesimally close trajectories is by definition governed by the dynamics in tangent space, finite size effects due to higher order terms can enter already on moderate length scales and thus yield different, usually larger, effective divergence rates than expected from the tangent space dynamics. In particular, when the maximal Lyapunov exponent is slightly negative (or zero), this can yield the puzzling observation that nearby trajectories might diverge fast though the solutions are supposed to be (marginally) stable.

In order to understand and characterize such behavior quantitatively, we will define a *scale dependent stability number* $s(\varepsilon)$, which in the limit of small scales converges towards the maximal Lyapunov exponent. Moreover, we show that solutions of such systems with strong nonlinear instability exhibit also temporal disorder and a kind of mixing.

II. FINITE SIZE PERTURBATIONS AND STABILITY NUMBER

In this paper we restrict ourselves to systems with discrete time, which can e.g. be considered as Poincaré maps of flows. Let $\vec{x}_{n+1} = \vec{f}(\vec{x}_n)$ be a dynamical system in a D-dimensional phase space and $\vec{\varepsilon}$ an initial perturbation. Then

$$\lambda = \lim_{t\to\infty} \lim_{|\vec{\varepsilon}|\to 0} \frac{1}{t} \ln \left(\frac{|\vec{f}^t(\vec{x}_0) - \vec{f}^t(\vec{x}_0 + \vec{\varepsilon})|}{|\vec{\varepsilon}|} \right) \tag{1}$$

$$= \lim_{t\to\infty} \frac{1}{t} \ln | \prod_{n=1}^{t} J(\vec{x}_n) \frac{\vec{\varepsilon}}{|\vec{\varepsilon}|} | \,, \tag{2}$$

where $J(\vec{x}_n)$ is the Jacobian of the map $\vec{f}$ at $\vec{x}_n$ and f^t denotes the tth iteration of f, is the maximal Lyapunov exponent with probability one [5].

This definition cannot be easily generalized to finite perturbations, e.g. by taking into account higher order terms in $\vec{\varepsilon}$ in Eq. 2, since the growth of finite perturbations cannot be characterized by local properties of $\vec{f}$ at the position of the unperturbed solution. Motivated by

---

*Also University of Oldenburg, Faculty of Physics, Department of Energy and Semiconductor Research algorithms measuring the divergence of nearby trajectories in time series analysis [3,4], we introduce a numerical concept for nonlinear stability analysis..

Let $\vec{u}(\vec{x}_n)$ be the unit vector pointing into the local tangent space $E_1(\vec{x}_n)$ of the maximal Lyapunov exponent [5], i.e. numerically $\vec{u}(\vec{x}_n) = \prod_{m=1}^{n} J(\vec{x}_m)\vec{\varepsilon}/|\prod_{m=1}^{n} J(\vec{x}_m)\vec{\varepsilon}|$ for sufficiently large n and almost every $\vec{\varepsilon}$. We then define the function $S(\varepsilon, t)$ by

$$S(\varepsilon,t) = \frac{1}{N}\sum_{n=1}^{N} \ln\left(\frac{1}{2}\sum_{i=+,-} |\vec{f}^t(\vec{x}_n) - \vec{f}^t(\vec{y}_{n,i})|\right) \qquad (3)$$
$$\text{with } |\vec{x}_n - \vec{y}_{n,\pm}| = \pm\varepsilon\vec{u}(\vec{x}_n) ,$$

where the $\vec{x}_n$ are distributed according to the natural invariant measure, e.g. stem from a long trajectory. For each given evolution time t we thus average over the distances between the position of a reference trajectory at that moment, emerging from $\vec{x}_n$, and the positions of two neighboring trajectories started at an initial distance ε in the direction of the local maximal Lyapunov vector. If these trajectories diverge according to an exponential law, the logarithm of this average yields a local finite time divergence rate multiplied by t. These local rates are averaged over the whole invariant set[1].

Following these and the more detailed arguments in [4], $S(\varepsilon, t)$ as a function of t possesses a linear increase, if the trajectory is chaotic and the initial ε is sufficiently small, its slope being the maximal Lyapunov exponent of the system. This statement is valid for every system in the limit of infinitesimal ε, but in practice also true for finite ε for all commonly studied chaotic model systems.

We condense this information in the *scale dependent stability number* $s(\varepsilon)$ by

$$s(\varepsilon) := \left.\frac{dS(\varepsilon,t)}{dt}\right|_{t=t_c} \text{ for suitable } t_c . \qquad (4)$$

Numerically, we will estimate the slope $s(\varepsilon)$ by $s_{t_1,t_2}(\varepsilon) = (S(\varepsilon,t_2) - S(\varepsilon,t_1))/(t_2 - t_1)$ for suitable t_1 and t_2. The ambiguity in the choice of t_c and t_1, t_2, respectively, will turn out to be irrelevant, as long as we guarantee that atypical behavior due to too small or too large t_c is excluded (see examples in Sec.III). In cases where we find a linear increase of $S(\varepsilon, t)$, $s(\varepsilon)$ is well defined and independent of t_c for a broad range of t_c (and of t_1 and t_2). If $S(\varepsilon, t)$ does not possess a linear regime, we nevertheless want to characterize its increase by a single number, and we cannot but fix t_1 and t_2 arbitrarily. The conclusions to be drawn from $s(\varepsilon)$ in such cases will not depend on their precise values. The vagueness in the definition circumvents an additional problem in higher dimensional systems: If we do not direct the initial perturbations into the most expanding direction (e.g. due to numerical ease), the growth of perturbations will undergo a transient, during which the perturbation aligns with the locally most expanding direction, such that the exponential stretching with the maximal exponent will be observed only after some time $t > 0$. Moreover, if perturbations grow according to a power law (marginally stable motion), this leads to finite slopes for $t_c = 0$ and zero slope for $t_c \to \infty$.

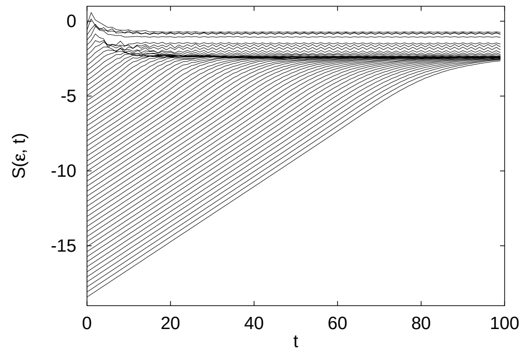

FIG. 1. $S(\varepsilon, t)$ for the chaotic circle map $\phi_{n+1} = \phi_n + \Omega + k \sin\phi_n$ with $k = 4.68$ and $\Omega = 4.8$.

In Fig.1 we show $S(\varepsilon, t)$ for the chaotic circle map, $\phi_{n+1} = \phi_n + \Omega + k\sin\phi_n$: As long as $S(\varepsilon, t) \lesssim -2$ we observe straight line segments, whose slope is approximately 0.186, the average Lyapunov exponent, independent of the initial neighborhood size ε. In the limit $\varepsilon \to 0$ one can follow the linear slope for $t \to \infty$, and we find exactly the Lyapunov exponent. For finite ε, the linear behavior terminates after finite times t, when saturation sets in.

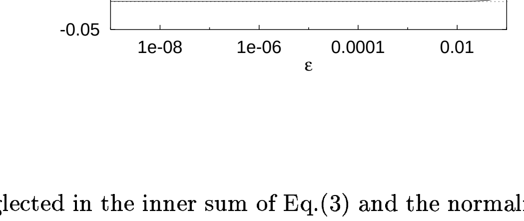

[1]Technical remark: If $\vec{y}_{n,\pm}$ lies outside the basin of attraction it is neglected in the inner sum of Eq.(3) and the normalization factor $\frac{1}{2}$ is accordingly corrected.

FIG. 2. The scale dependent stability number, numerically approximated by $s_{2,10}(\varepsilon)$, for chaotic solutions ($k = 4.68$, $\Omega = 4.68$) (obtained from the curves of Fig.1), for quasi-periodic solutions ($k = 0.4$, $\Omega = 4.68$) and for stable periodic solutions ($k = 0.4$, $\Omega = 0.674\pi$) of the circle map (from top to bottom). The values of the maximal Lyapunov exponent 0.186, 0 and -0.022 found from the tangent space dynamics, $\lambda = \langle \ln |f'(x_t)| \rangle$, agree well.

The upper curve of Fig.2 shows the scale dependent stability number, derived from the information of Fig.1. The signature is typical of a "well-behaved" chaotic system (such as also e.g. the Hénon map, the Ikeda map, the Poincaré map of the Lorenz system): Apart from the saturation effects on scales comparable to the overall size of the attractor and an overestimation due to second order effects on slightly smaller scales, we see a good agreement between $s(\varepsilon)$ and the Lyapunov exponent $\lambda \approx 0.186$ (dotted line) even for large ε.

For quasi-periodic solutions of the circle map (here: $k = 0.4$, $\Omega = 4.68$ = golden mean $\times\ 2\pi$), we obtain horizontal lines for $S(\varepsilon, t)$ and $s(\varepsilon) = 0$ for all ε (Fig.1), again in perfect agreement with the linear stability analysis. Finally, if the maximal Lyapunov exponent is negative (and the solution a periodic orbit), we faithfully obtain negative slopes which again are identical to the value of the Lyapunov exponent.

Thus the finite scale stability number $s(\varepsilon)$ does not only converge towards the maximal Lyapunov exponent of the system in the limit of $\varepsilon \to 0$ by construction, but additionally represents its value also on larger scales, if the tangent space dynamics also governs finite size perturbations.

III. QUASI CHAOS: NONLINEAR INSTABILITY DESPITE LINEAR STABILITY

In this section we will discuss three classes of systems, where the scale dependent stability number gives insight into a kind of temporal disorder without positive Lyapunov exponents.

A. Discontinuous maps

The behavior of maps with a large number of discontinuities can be very different on infinitesimal scales and on scales related to the distance between the discontinuities. Let us approximate the circle map,

$$x_{n+1} = f_c(x_n) = x_n + \Omega + k \sin(x_n)\ , \tag{5}$$

by a piecewise linear map of M pieces, by interpolating linearly between $f_c(x = n2\pi/M)$ and $f_c(x = (n+1)2\pi/M)$. Then, in order to introduce discontinuities, we reflect each linear piece at its midpoint. The map thus reads:

$$f(x) = y_{n+1} + (x - z_n)\frac{y_n - y_{n+1}}{z_{n+1} - z_n}, \quad x \in [z_n, z_{n+1}], \tag{6}$$

where $z_n = n2\pi/M$ and $y_n = f_c(z_n)$. If we consider the case $k < 1$, this map is one-to-one and it thus cannot have chaotic solutions (no possibility for mixing). Instead, all solutions must be quasi-periodic or periodic. In fact, for many values of M, Ω and k we find, after some transient, periodic motion of short periods and with negative Lyapunov exponents. Nevertheless, one can focus on parameters k and Ω (e.g. $k = 0.4$, $\Omega = 4.68$) for which a trajectory has not yet locked into a periodic solution after 20000 iterations. Such orbits create invariant measures which are practically ergodic on the interval $[0 : 2\pi]$. In these cases, the numerical value of the Lyapunov exponent, $\lambda = \langle \ln |f'(x_t)| \rangle$, is statistically consistent with 0.

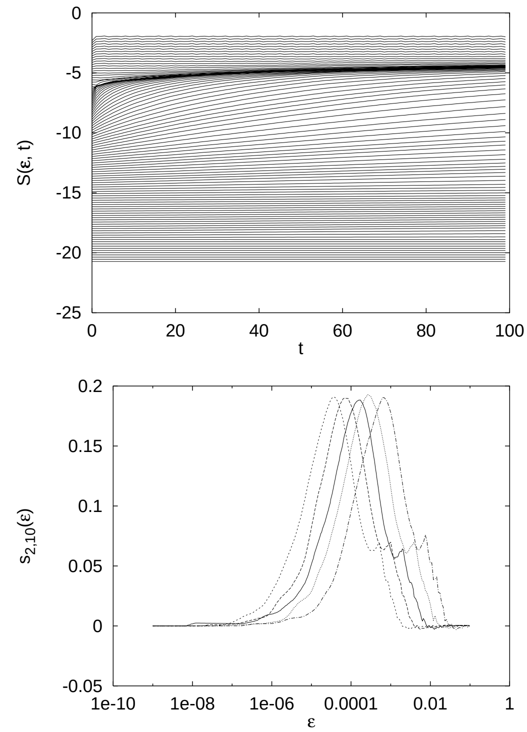

FIG. 3. Quasichaos in the piecewise linear discontinuous circle map (M=500): $S(\varepsilon, t)$ (upper panel) and $s_{2,10}(\varepsilon)$ (lower panel, continuous curve). Additional dotted curves in the right panel show the dependence on the discretization length scale of the map Eq.6, $M = 125$, $M = 250$, $M = 1000$, $M = 2000$ from right to left.

The functions $S(\varepsilon, t)$ and $s_{2,10}(\varepsilon)$ (Fig.3), however, differ strongly from the behaviour reflected by Figs.1-2. For $M = 500$ we see that above a value $\varepsilon_u \approx 0.01$ all lines are almost horizontal, reflecting a zero exponent. Below ε_u, the situation changes drastically: the average distance increases very fast and saturates around ε_u. The divergence rate becomes the lower the smaller ε, and below $\varepsilon_l \approx 10^{-6}$ all lines are practically horizontal again.

In the range of ε where the curves $S(\varepsilon, t)$ are no clear straight line segments before saturation, the precise values of $s(\varepsilon)$ do depend on t_1 and t_2 used to estimate the slope of $S(\varepsilon, t)$. Nevertheless, as said before, the conclusions to be drawn from it will not depend on precise values. The curve $s_{2,10}(\varepsilon)$ well represents the essentials of $S(\varepsilon, t)$: There is marginal stability on the very small scales (in agreement with $\lambda = 0$) and on the large scales, and strong instability on intermediate scales. This instability becomes, during very short times, extremely large, due to the large slopes of the initial parts of $S(\varepsilon, t)$ around $S(\varepsilon, 0) = \ln \varepsilon \approx -7$. In the scale dependent stability number this is reflected by the maximum around $\varepsilon \approx 10^{-4}$. The maximum value of $s(\varepsilon)$ is only implicitly related to properties of the system, more precisely, to its discontinuities. When ε is large compared to the length scales introduced by the discretization, the increase of distances is governed again by linear stability analysis, but now by the one corresponding to the smooth analogue of our map which in this case is the non-chaotic circle map.

The left part of $s(\varepsilon)$, the approach towards $s = 0$ for decreasing ε, can be determined by the following arguments: We have checked that the points of the reference trajectory are almost uniformly distributed inside each interval of length $1/M$. Let us consider those points inside this interval, whose ε-neighbours (denoted by $y_{n,\pm}$ in Eq.(3)) are located in one of the two adjacent intervals. The fraction of these points is $2M\varepsilon$. The average height of the discontinuities is $2/M$, and, under the approximation that the slopes are almost the same in both intervals, this is also the distance between the image of such a point and the image of its ε-neighbour. Thus for $\varepsilon < \frac{1}{M}$ we find $s_{0,1}(\varepsilon) = 2M\varepsilon \ln \frac{1}{M\varepsilon}$. This behaviour is in fact well represented by the numerical results (see Fig.4).

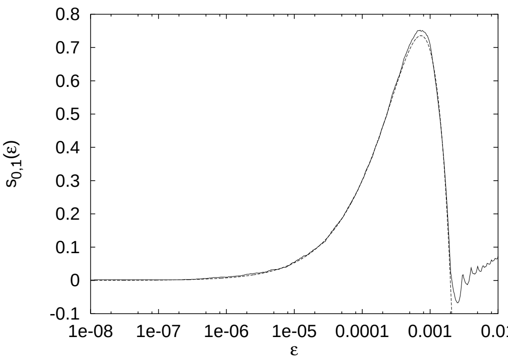

FIG. 4. $s_{0,1}(\varepsilon)$ for the piecewise linear discontinuous circle map ($M = 500$, $k = 0.4$, $\Omega = 4.68$) (continuous curve) and the predicted values (dashed curve).

The dependence of ε_u and the location of maximal instability on the number the discontinuities and thus on the size of the intervals between jumps and their heights is also shown in Fig.3 (lower panel, dotted curves): $\varepsilon_u \propto 1/M$, as expected from our arguments.

The notion of quasi-*chaos* is not just based on the positivity of the scale dependent stability number in some range of length scales, but is also justified from other points of view, since such dynamics exhibits temporal disorder. In Fig.5 we compare the power spectra of the circle map and its quasi-chaotic version, Eq.(5) and Eq.(6). Whereas the spectrum of the circle map shows the well known features of quasiperiodic motion, the spectrum of the quasi-chaotic system has a broad-band background, many peaks disappeared and the remaining peaks are broadened, as it is typical of chaotic motion with a strong (quasi-)periodic component. Moreover, when plotting e.g. every 27th data point of a typical trajectory, we observe clear disorder in the quasichaotic system (Fig.6).

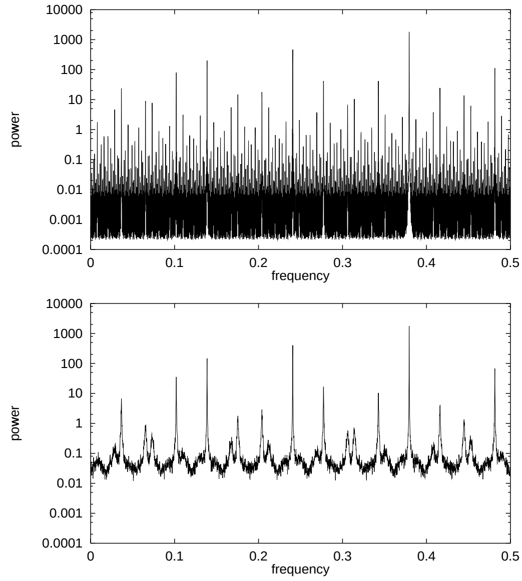

FIG. 5. Power spectra of the circle map and its quasi-chaotic counterpart for $k = 0.4$ and $\Omega = 4.68$.

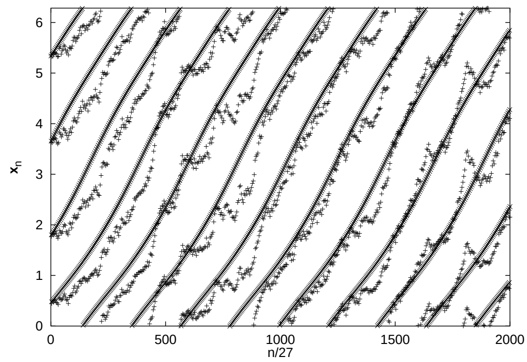

FIG. 6. Time series of the circle map ($\times$) and its quasi-chaotic counterpart (+), plotting only every 27th value.

Since our map is one-dimensional and invertible, there cannot be mixing and thus no true chaos. Instead, we find very long attractive periodic orbits, preceded by even longer transients. The basin of attraction is very complicated and creates a situation which, when seen in a coarse rained way, looks like mixing: In contrast to real mixing, $\lim_{t\to\infty} \mu(f^t(A) \cap B) = \mu(A)\mu(B)$ is only fulfilled for subsets A and B of the state space with a sufficiently large diameter.

The latter aspects are more conveniently studied for an even simpler map, where all slopes of the linear pieces are identical to unity. We will present detailed results about the properties of such a system, a Bernoulli map with random additional discontinuities, in a separate paper [6].

B. A coupled map lattice

Politi et. al. [7] studied a spatially extended system showing strong spatio-temporal disorder during some transient whose length grows exponentially with system size. The puzzling observation was, however, that even during this disordered transient, the maximal Lyapunov exponent is strictly negative.

The system, a coupled map lattice, reads

$$x^i_{n+1} = (1-2\sigma)f(x^i_n) + \sigma\Big(f(x^{i+1}_n) + f(x^{i-1}_n)\Big)$$
$$f(x) = \begin{cases} bx, & 0 < x < 1/b, \\ a + c(x - 1/b), & 1/b \le x < 1. \end{cases} \quad (7)$$

For a=0.07, b=2.7, c=0.1 the uncoupled map possesses a stable period-three orbit with elements $\{0.121, 0.328, 0.887\}$, which is also the most probable asymptotic solution of the CML with coupling $\sigma = 1/3$. Through the strong contraction of f on the right interval, even the Lyapunov exponent of a disordered transient is negative. Its value is relatively robust against changes of the initial condition, and, due to the flatness of the Lyapunov spectrum, is almost independent of the system size. In Fig.7 we show the $S(\varepsilon, t)$ curves for N=25 maps and the $s(\varepsilon)$-curves for several systems sizes, all obtained on trajectories of length 1000 which were fully in the disordered transient state. In the limit of infinitesimal perturbations, we find a very good agreement with the numerically determined maximal Lyapunov exponents $\lambda_1 \approx -0.123$ and $s(\varepsilon)$ only if t_c is very large. For numerical ease we have chosen random initial perturbations. Therefore we observe finite time deviations in Fig.7, because of the small value of $\lambda_1 - \lambda_2$. However, what is more important, we see that perturbations which are larger than about 0.01 grow with time! We thus conjecture that the instability which leads to the spatiotemporal disorder is this sensitivity to finite size perturbations, which are permanently acting onto each individual map through the coupling to its neighbors. As we saw in the modified circle map, this kind of instability is well able to create motion which looks disordered.

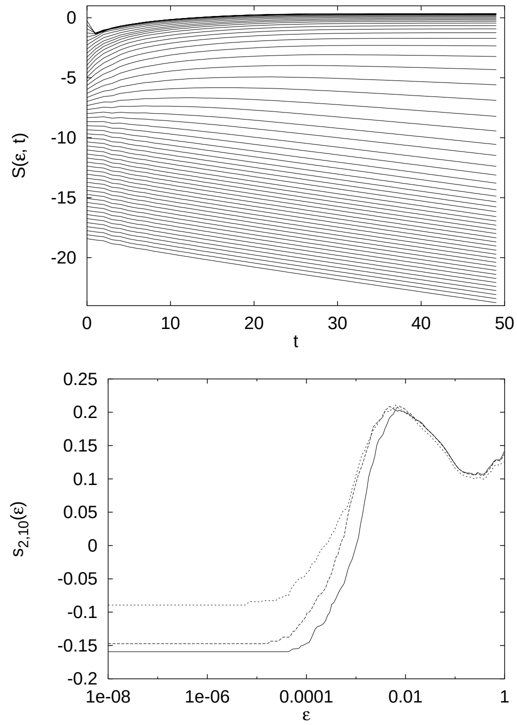

FIG. 7. $S(\varepsilon, t)$ for the 25-dim coupled map lattice (upper panel) and $s_{2,8}(\varepsilon)$ for 20-dim, 25-dim, 30-dim (lower panel, from bottom to top).

C. Polygonal billiards

Billiards have been extensively studied in connexion with the quantization of chaotic systems, but here we will discuss the classical motion of a free particle confined to some region of space by ideally reflecting boundaries. The equation of motion is thus trivial inside the billiard and is governed by the simple reflection law when the particle hits the boundary. The natural time discrete dynamical system is given by the map from one reflection point to the next one. We will study regular polygonal billiards inscribed in the unit circle. The coordinates we use are thus (ϕ_i, α_i), where ϕ_i is the angle of radius vector through the reflection point, measured with respect to the horizontal, and α_i is the angle of the reflected particle, also measured with respect to the horizontal (see Fig.8).

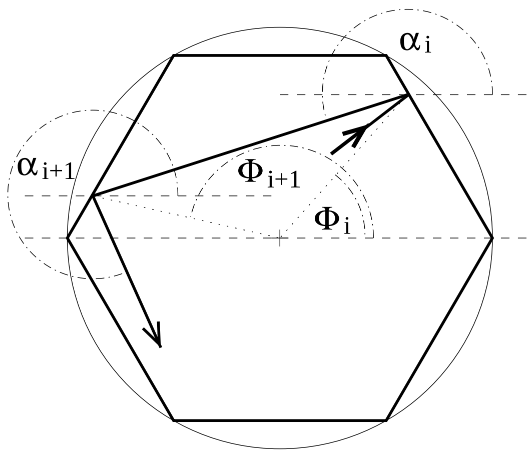

FIG. 8. A hexagonal billiard with a short part of a trajectory and our notation of the coordinates.

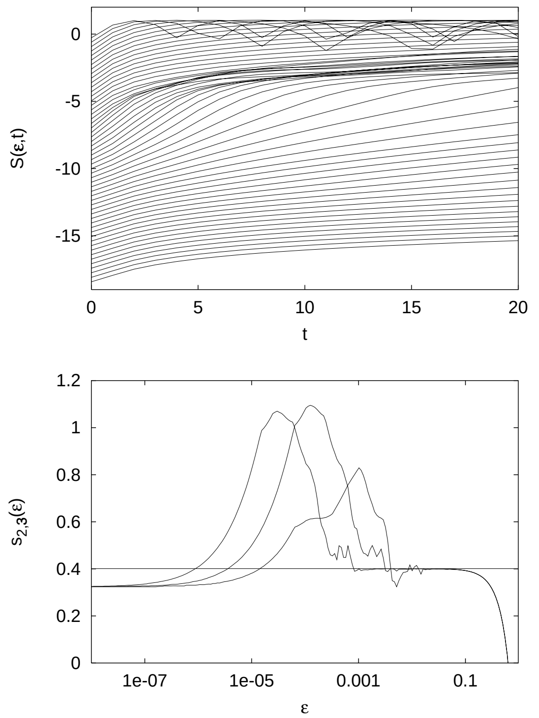

FIG. 9. The function $S(\varepsilon, t)$ (upper panel) and the scale dependent stability number $s_{2,3}(\varepsilon)$ (lower panel) for regular polygonal billiards with edge numbers N=500, 2000, and 8000 (curves from right to left).

Billiards with boundaries formed by straight lines were studied thoroughly and termed quasi-integrable, almost integrable etc., since infinitesimally close trajectories can only diverge linearly in time and solutions are thus marginally stable [8]. Despite this fact, in [9] it was observed that typical solutions exhibit temporal disorder, and the comparison of nearby trajectories allowed them to measure a positive Lyapunov exponent even for regular polygons, which approximate the integrable circular billiard. We therefore conduct our nonlinear stability analysis for these systems. In Fig.9 we show the scale dependent stability numbers obtained by numerical simulation of billiards with different edge numbers. On the large scales, the behavior of a polygonal billiard is indistinguishable from a circular billiard. Trajectories diverge linearly in time, i.e. the motion is marginally stable but algebraically unstable, in contrast to the circle map. Thus here the t_c of Eq.(2) should be large in order to find the correct Lyapunov exponent $\lambda = 0$. Instead, we translate this instability into the stability number $s(\varepsilon)$ through the slope of the law $S(\varepsilon, t) = log(at+b)$, where a and b are constants given by the initial separation of the trajectories and the rate of the linear divergence of the trajectories, on the appropriate time interval. A very similar result also holds in the limit of very small ε. Here, the perturbations are small compared to the edge lengths of the polygons, and again the perturbations increase linearly with the number of reflections. However, when compared to the circular case, here only half of the perturbations leads to this linear instability due to the fact that a mere translation of the reflection point has low probability to lead to a divergence of the trajectories in the first time step. One can compute the $S(\varepsilon, t)$-curves for both this limit and the circular billiard analytically and derive the values of $s_{2,3}(\varepsilon)$, $\ln(\frac{\sqrt{85}+\sqrt{61}}{2}) - \ln(\frac{\sqrt{41}-\sqrt{25}}{2})$ for the circular billiard, which is indicated in Fig.9. On intermediate length scales, however, one observes a strong instability, which occurs when the initial perturbation is of the order of the size of the edge lengths. Nonlinear stability analysis thus reveals that this marginally stable system whose macroscopic approximation is also marginally stable possesses sensitivity to perturbations of the order of magnitude of $1/N$, where N is the number of edges. We have thus clear evidence that the positive Lyapunov exponent determined in Ref. [9] is a misinterpretation, perhaps because of an unsuitable choice of the range of length scales in which the instability was measured.

IV. SUMMARY

We have introduced the concept of stability with respect to finite size perturbations, condensed in the quantity $s(\varepsilon)$, the scale dependent stability number, which in the limit $\varepsilon \to 0$ converges towards the maximal Lyapunov exponent. We have demonstrated that for certain classes of dynamical systems this concept provides a more detailed description of the system's response to perturbations than the linear stability analysis, including the possibility for strong instability despite zero or negative Lyapunov exponents. Moreover, there is evidence, that such a kind of instability can lead to solutions which are aperiodic and show temporal disorder.

Quasi-chaos seems to be common to systems with discontinuities, although we have also found this behavior in continuous 1-d maps with large second derivatives (not shown in this paper). Since in technical environments, in particular in control systems, piecewise linear discontinuous functions are ubiquitous, we expect this phenomenon to be of considerable relevance. We discussed polygonal billiards as a physically motivated system of this type.

The notion of pseudo-chaos has gained recent interest in an article of Chirikov and Vivaldi [10]. Starting from the relationship between quantum and classical dynamics, they discuss systems where exponential instability on infinite times is prohibited by the discreteness of the state space. In view of this it is puzzling, that in the systems of our paper the discreteness of the dynamics introduced by the discontinuities gives rise to instabilities, even if the corresponding smooth dynamics on the infinitesimal scales and in the macroscopic limits are marginally stable.

Recently, in two very interesting papers a finite size Lyapunov exponent was introduced [11,12]. This exponent was designed to investigate chaotic systems with separation of time and length scales and differs from this work in both scope and method. In particular, since it relies on error doubling times, it cannot be used to determine zero or negative expansion rates.

ACKNOWLEDGEMENTS

We thank P. Grassberger, R. Livi, and A. Politi for stimulating discussions, which where enabled by the kind hospitality of ISI, Torino, and financial support from EC under grant No. ERBCHRX-CT940546.

[1] H. Kantz, T. Schreiber, *Nonlinear Time Series Analysis*, Cambridge University Press, 1997

[2] A. Wolf, J. B. Swift, L. Swinney and A. Vastano, Pysica D 16 (1985) 285.

[3] M. T. Rosenstein, J. J. Collins, C, J. de Luca, Pysica D 65 (1993) 117.

[4] H. Kantz, Physics Letters A 185 (1994) 77.

[5] J. P. Eckmann and D. Ruelle, Rev. Mod. Phys. 57 (1985) 617

[6] H. Kantz and T. Letz *Instability of non-chaotic systems with many discontinuities*, in preparation.

[7] A. Politi, R. Livi, G.-L. Oppo, R. Kapral, Europhys. Lett., 22 (8) 571 (1993)

[8] E. Gutkin, *Billiards in polygons*, Physica **19D**, 311-333 (1986); E. Gutkin, *Billiards in polygons: Survey of recent results*, J. Stat. Phys. **83**, 7-26 (1996).

[9] J.L. Vega, T. Uzer, J. Ford, *Chaotic billiards with neutral boundaries*, Phys. Rev. **E48**, 3414-3420 (1993).

[10] B.V. Chirikov and F. Vivaldi, Physica **D 129**, 223-235 (1999).

[11] E. Aurell, G. Boffetta, A. Crisanti, G. Paladin, A. Vulpiani, *Predictability in the large: an extension of the concept of Lyapunov exponent*, J. Phys. A **30**, 1 (1997).

[12] G. Boffetta, A. Crisanti, F. Paparella, A. Provenzale, A. Vulpiani, *Slow and fast dynamics in coupled systems: A time series analysis view*, Physica D **116**, 301 (1998).